6038 *Macromolecules* **2009**, *42*, 6038–6043
DOI: 10.1021/ma9009017

Macromolecules
ARTICLE

High-Performance Carboxylated Polymers of Intrinsic Microporosity (PIMs) with Tunable Gas Transport Properties[†]

Naiying Du,[‡] Gilles P. Robertson,[‡] Jingshe Song,[‡] Ingo Pinnau,[§] and Michael D. Guiver*[,‡]

[‡]*Institute for Chemical Process and Environmental Technology, National Research Council of Canada, Ottawa, Ontario K1A 0R6, Canada, and* [§]*Membrane Technology and Research, Inc., 1360 Willow Road, Suite 103, Menlo Park, California 94025-1516*

Received April 24, 2009; Revised Manuscript Received June 1, 2009

ABSTRACT: Carboxylated polymers of intrinsic microporosity (carboxylated PIMs) are reported as potential high-performance materials for membrane-based gas separation. Carboxylated PIM membranes were prepared by in situ hydrolysis of the nitrile groups of PIM-1 films. Structural characterization was performed by Fourier transform infrared spectroscopy (FTIR) and proton nuclear magnetic resonance (^{1}H NMR). The degree of hydrolysis was determined by carbon elemental analysis. The thermal properties were evaluated by differential scanning calorimetry (DSC) and thermogravimetric analysis (TGA). Compared with PIM-1, carboxylated PIMs with different degrees of hydrolysis have similar thermal and mechanical properties but show higher selectivity for gas pairs such as O_2/N_2, CO_2/N_2, He/N_2, and H_2/N_2 with a corresponding decrease in permeability. Selectivity coupled to high permeability combines to exceed the Robeson upper-bound line for the O_2/N_2 gas pair. This work demonstrates that significant improvements in gas separation properties may be obtained through postmodification of nitrile-based PIM membranes. The present work improves the understanding of the relationship of structure/permeation properties and also extends the PIM spectrum beyond those reported previously. In addition, the incorporation of carboxylic acid sites has the potential for further modification reactions such as grafting and cross-linking.

Introduction

Microporous materials (pore size < 20 Å) are of great technological importance for adsorption, separation, and heterogeneous catalysis because of their large and accessible surface areas (typically 300−1500 m^2/g). Two main classes of inorganic microporous materials, zeolites (aluminosilicate) and activated carbons, are widely used in industry. In addition, extensive research has been carried out in the last 10 years to produce intrinsically microporous polymeric materials.[1−12] These novel polymers mimic the microporous structure of inorganic materials but also offer numerous advantages, such as good processability, broader range of physical properties, and potential for introducing functionality. During the last four years, the groups of Budd and McKeown[13−17] have reported dioxane-based ladder polymers of intrinsic microporosity (PIMs), which possess an amorphous microporous glassy structure with good processability. These PIMs derive their properties from their highly rigid and contorted ladder structures, which can prevent efficient chain packing and offer extraordinarily high surface areas. Because of the initial reports of Budd and McKeown, other groups have broadened this work to explore different polymerization techniques or produce structurally different PIMs, which maintain high permeability (e.g., oxygen permeability, $P_{O2} > 100$ barrer) combined with a selectivity that often exceeds the Robeson upper bound. However, only a few such polymers have been reported that provide robust, high-molecular-weight materials for gas permeability measurements[13,18−20] because of the lack of suitably reactive monomers for polycondensation.

In our previous work, monomers were synthesized for the preparation of structurally new PIMs, whereby gas permeability, selectivity, and other properties were tuned to adjust the interchain spacing and to enhance the chain rigidity.[20,21] Although several high-molecular-weight PIMs were recently prepared by polycondensation of new synthetic monomers, the present postmodification approach provides an alternative route to new PIM materials. In the present work, we report details of a simple postmodification hydrolysis reaction, which converts the nitrile groups in PIM-1 to carboxyl groups, providing structurally new PIM materials. The gas permeation properties of the carboxylated PIMs, which can be controlled by hydrolysis conditions, are reported and discussed with respect to the degree of hydrolysis.

Experimental Section

Materials. Dimethylacetamide (DMAc, Sigma-Aldrich), toluene (Sigma-Aldrich), methanol (MeOH, Sigma-Aldrich), sodium hydroxide (Sigma-Aldrich), and chloroform (Sigma-Aldrich) were used as received. 5,5′,6,6′-Tetrahydroxy-3,3,3′,3′-tetramethylspirobisindane (TTSBI, Sigma-Aldrich) was purified by crystallization from methanol. Tetrafluoroterephthalonitrile (TFTPN, Matrix Scientific) was purified by vacuum sublimation at 150 °C under an inert atmosphere.

Characterization Methods. The structures of the polymeric materials were fully characterized using nuclear magnetic resonance (NMR) spectroscopy at different temperature. NMR analyses were recorded on a Varian Unity Inova spectrometer at a resonance frequency of 399.961 MHz for ^{1}H and 376.276 MHz for ^{19}F. ^{1}H and ^{19}F NMR spectra were obtained from samples dissolved in $CDCl_3$ or DMSO-d_6 using a 5 mm pulsed field gradient indirect detection probe. The solvent signals ($CDCl_3$ ^{1}H 7.25 ppm; DMSO-d_6 ^{1}H 2.50 ppm) were used as the internal references. An external reference was used for ^{19}F NMR/$CFCl_3$ 0 ppm.

[†] NRCC publication no. 51691.
*Corresponding author. E-mail: michael.guiver@nrc-cnrc.gc.ca.

 Published on Web 06/24/2009

Scheme 1. Reaction Scheme for Hydrolysis of PIM-1

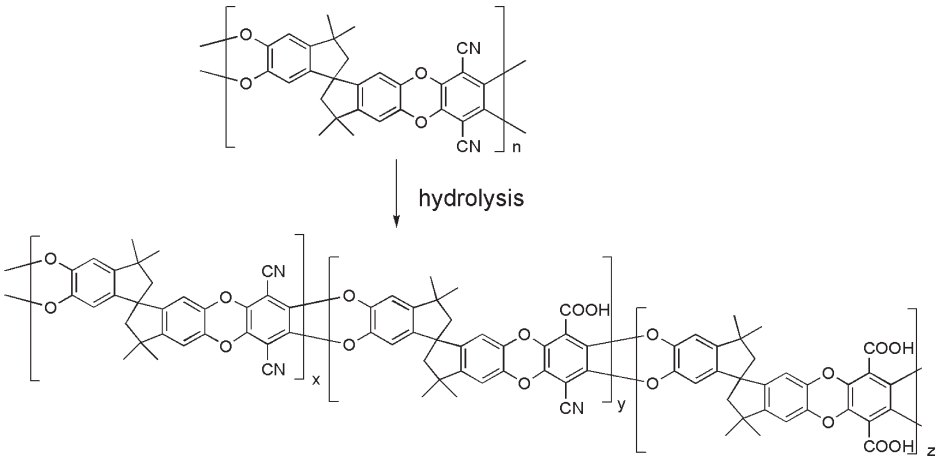

Molecular weight and molecular weight distributions were measured by GPC using Ultrastyragel columns and THF as the eluent at a flow rate of 1 mL/min. The values obtained were determined by comparison with a series of polystyrene standards.

FTIR (Fourier transformed infrared) spectra were recorded on a Perkin-Elmer FTIR microscope with film samples at 8 cm^{-1} resolution over the 400−4000 cm^{-1} range. Each sample was scanned 50 times.

Elemental analysis was carried out with a Thermoquest CHNS-O elemental analyzer. Polymer thermal degradation curves were obtained from thermogravimetric analysis (TGA) (TA Instruments model 2950). Polymer samples for TGA were initially heated to 120 °C under nitrogen gas (50 mL/min) and maintained at that temperature for 1 h for moisture removal and then heated to 600 at 10 °C/min for degradation temperature measurement. Glass-transition temperatures (T_g) were observed from DSC (TA Instruments model 2920), and samples for DSC were heated at 10 °C/min under a nitrogen flow of 50 mL/min and then quenched with liquid nitrogen and reheated at 10 °C/min for the T_g measurement.

Dense polymer films for gas permeability measurements were prepared from 1 to 2 wt % PIM-1 solutions in chloroform. PIM-1 solutions were filtered through 0.45 μm polypropylene filters and then cast into Teflon Petri dishes in a glovebox and allowed to evaporate slowly for 1 day. The membranes were soaked in methanol and dried in a vacuum oven at 100 °C for 24 h. The resulting membranes with thickness in the range of 70−90 μm were bright-yellow and flexible. The absence of residual solvent in the membranes was confirmed by weight-loss tests using TGA. The PIM-1 membranes were soaked in 20 wt % sodium hydroxide solution (H_2O/ethanol = 1:1). After hydrolyzing at different temperatures for different hydrolysis times, the membranes were boiled in water (with a few drops of HCl, pH 4 to 5) for 2 h. Following several washing cycles in water, the membranes were soaked in methanol for 1 h and then allowed to dry at ambient temperature. Finally, the membranes were dried in a vacuum oven for 24 h by gradually increasing the temperature from ambient to 100 °C.

Permeability coefficients (P) of N_2, O_2, He, H_2, and CO_2 were determined at 25 °C at a feed pressure of 50 psig and atmospheric permeate pressure using the constant-pressure/variable-volume method. The permeation flow was measured using a bubble flow meter, with the exception of CO_2, which was measured by a mass flow meter (Agilent ADM 2000). P was calculated by using the following equation

$$P = \left(\frac{273}{T}\right)\left(\frac{dV}{dt}\right)\left(\frac{l}{\Delta pA}\right)$$

(1)where dV/dt is the permeate-side flow rate and T is the operation temperature (K). The membrane effective area was 9.6 cm^2.

Results and Discussion

Although hydrolyzed PIM-1 has been mentioned as a possible hydrolysis product in a patent application,[15] no details regarding hydrolysis procedures, characterization of the main chain structure, and gas separation properties were reported. In the present work, the PIM-1 starting material used for the hydrolysis experiments was gel-free and had high molecular weight (M_n = 50 000, PDI = 2.0), which was obtained under an optimized polycondensation process.[20] Scheme 1 shows possible resulting repeat units derived from different degrees of hydrolysis. Polymer repeat units may contain zero, one, or two nitrile groups and correspondingly have two, one, or zero carboxylic acid groups.

At low temperatures (25 and 65 °C), the hydrolysis reaction occurred rapidly during the initial stage but slowed down after 24 h, as demonstrated by FTIR and ^{1}H NMR measurements. At elevated temperature (reflux at 120 °C), the hydrolysis reaction was complete within 5 h. The resulting fully carboxylated PIM (120 °C, 5 h) was characterized by ^{1}H and ^{19}F NMR spectroscopy. Stacked ^{1}H NMR spectra of PIM-1 in $CDCl_3$ and carboxylated PIM in DMSO-d_6 (120 °C, 5 h) are displayed in Figure 1 along with peak assignments derived from 2D-NMR.

The intensities and the shapes of the carboxylated-PIM polymer ^{1}H NMR signals were monitored at different NMR probe temperatures: 50, 85, 100, and 120 °C. The observed peak intensity ratio for the aromatic (5.75−8.50 ppm, H-6, 9 and COOH) and aliphatic (0.25 to 2.4 ppm, H-2 and CH_3) regions was exactly 6H: 16H as expected from the molecular structure. Furthermore, the broad peaks in the 7.1 to 8.5 ppm area changed shape with increasing temperature. It is well known in NMR spectroscopy that changes in the sample temperature will affect the mobility of the molecules and hence the shape of the signals. This is particularly noticeable with protons involved in hydrogen bonding (exchange rate, electron density around the H nuclei),[22a] whereas other aromatic and aliphatic protons are often left unchanged. The spectra of Figure 1 are a good example of what can happen to the shape and shift of −COOH proton signals while H-bonding is affected by temperature changes. Increased temperature disrupts the hydrogen bonding and gradually shifts the −COOH signals to lower frequencies (less H-bonding). A drop of D_2O was added to the tube, and its immediate effect was observed in the ^{1}H NMR spectrum (Figure 1). The −COOH protons exchanged with the deuterium nuclei of D_2O and hence proved the presence of labile protons from the −COOH groups.

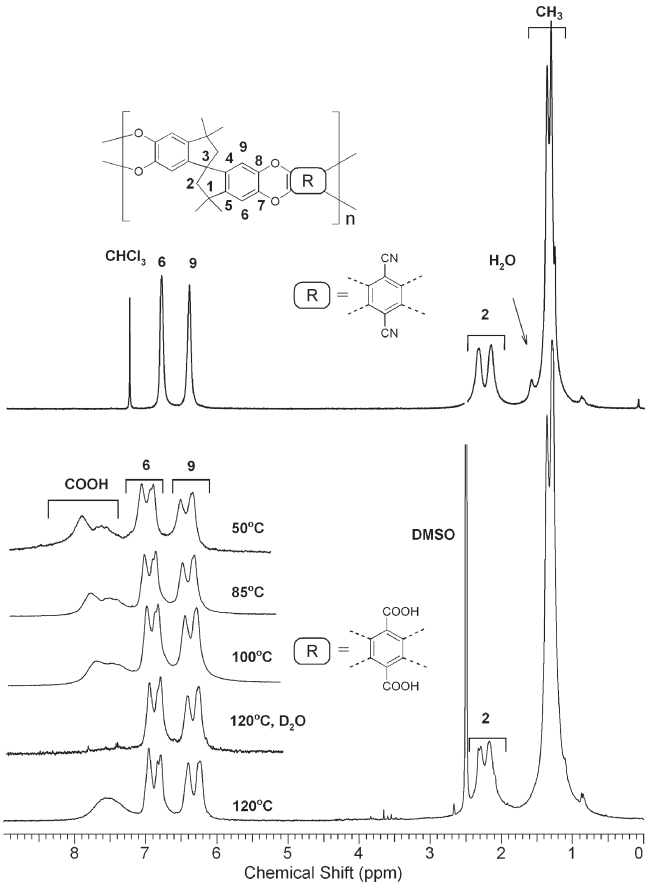

Figure 1. ^{1}H NMR spectra of PIM-1 and fully carboxylated PIMs (120 °C, 5 h).

It is worth mentioning that the full spectrum of carboxylated PIM displayed in Figure 1 (120 °C) was acquired with a water suppression pulse sequence that resulted in the absence of a water peak at 3.7 ppm. Finally, the polymers were scanned for ^{19}F NMR signals, and no fluorine atoms were detected. The FTIR spectra of the progress of hydrolysis at 120 °C at different reaction times to produce carboxylated-PIM membranes are shown in Figure 2.

PIM-1 (0 h) shows the characteristic nitrile absorption band at 2238 cm^{-1}, whereas the absence of absorption bands in the range of 3000 to 3600 cm^{-1} indicates that no carboxylic acid group is present. After a 1 h hydrolysis reaction time at 120 °C, the relative intensity of the nitrile absorption band decreased compared with that of other bands. Broad strong absorptions comprising three bands are observed in the range of 3000 to 3600 cm^{-1}, corresponding to O−H stretching vibrations. A narrow intense absorption near 1700 cm^{-1} arises because of stretching vibration of the C═O group. These combined bands imply that some of the nitrile groups were converted into carboxylic acid groups. It is notable that the three bands in the range of 3000 to 3600 cm^{-1} represent three possible types of O−H stretching vibrations in carboxylated-PIM membrane: free carboxylic acid structure (3500 cm^{-1}), hydrogen-bonded carboxylic acid dimers (3300 cm^{-1}), and O−H hydrogen-bonded with dioxane (3100 cm^{-1}).[22b] This result is consistent with ^{1}H NMR results but provides more detail. In addition, absorption near 1600 cm^{-1} is observed in carboxylated PIMs and PIM-1 but is quite weak in PIM-1. It is presumed that this band is composed of the stretching vibrations of C═O and aromatic C−C. The C═O band is shifted to lower frequencies (from 1700 to 1600 cm^{-1}) than those observed for free carboxylic acid due to strong hydrogen bonding. In addition, it is also considered that the intensity of the aromatic C−C band

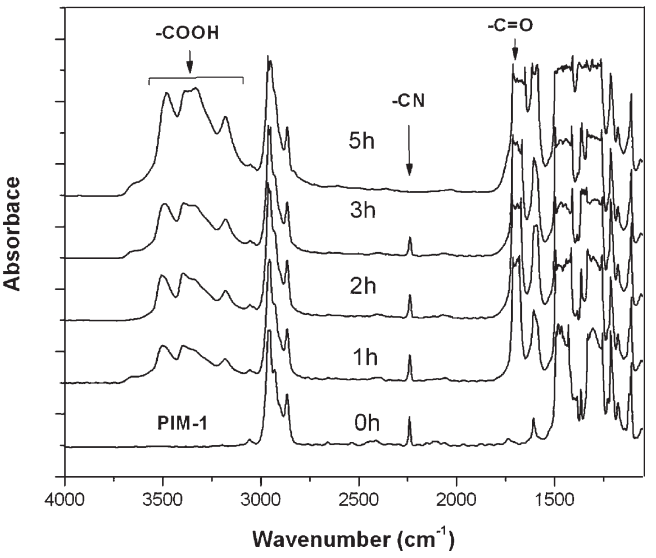

Figure 2. FTIR spectra of PIM-1 membrane and carboxylated-PIMs membranes (hydrolysis time of PIM-1: 0, 1, 2, 3, and 4 h).

might increase because the center of symmetry in the aromatic ring is generally weaker in carboxylated benzene than in the one containing nitrile.[22,23] To prove that nitrile groups were converted into carboxylic acid groups, the hydrolysis reaction time was extended. The relative height of the C═O carboxylic acid absorption band increased obviously, and the nitrile absorption band decreased until it disappeared after a 5 h reaction time, indicating that nitrile groups were completely hydrolyzed into carboxyl groups.

In general, the intensities of −CN absorption bands can be used to calculate the approximate degree of hydrolysis. However, in the particular case of PIM-1 hydrolysis, where two symmetrical para-substituted −CN groups occur, symmetrical −CN groups have different intensities than those of asymmetrical −CN groups, which would occur after hydrolysis. Therefore, the degree of hydrolysis cannot be conveniently determined quantitatively by FTIR spectra. However, a relationship between the degree of hydrolysis and the carbon content of the polymer can be conveniently established using the following equation

$$C = \frac{348.3}{460.48+38H}, \quad \text{which can be rewritten}$$

$$H = \frac{(348.3-460.48C)}{38C}$$

where C is the carbon content and H is the degree of hydrolysis. A standard calibration line obtained by calculation is plotted in Figure 3.

The carbon content of the carboxylated PIMs can be detected by elemental analysis; therefore, the degree of hydrolysis can be ascertained from the line. Because carboxylated PIM is prone to water absorption from ambient air, the measured carbon content could be somewhat lower than the actual one, which would result in a slightly lower degree of hydrolysis values. Nevertheless, this method appears to be a feasible way to determine the degree of hydrolysis and was much more effective than nitrogen analysis. As seen from Figure 3 and Table 1, the hydrolysis reaction is very fast at elevated temperature. At 120 °C, 67% −CN was hydrolyzed within 3 h. It is also shown that around 90% −CN was converted into −COOH after 5 h. However, at low temperature, the reaction proceeds more slowly, and the degree of hydrolysis is still quite low even after a prolonged reaction time.

These results are in good agreement with ^{1}HNMR and FTIR results. The reason that the hydrolysis reaction proceeds more slowly than the initial reaction can be explained plausibly by the FTIR spectra. The hydrolysis of some of the nitrile groups to carboxylic acid groups provides the conditions for dimer formation because of strong hydrogen bonding of −COOH groups or intermolecular hydrogen bonding of −OH with dioxane, which leads to the build up of an impermanent network, as depicted in Figure 4. This could retard access of the hydrolysis reagent (sodium hydroxide or other base and solvent) into the polymer membrane or material. At elevated temperatures, the hydrogen or intermolecular bonds are weaker and the network is broken such that the hydrolysis reagent can access the nitrile groups more easily, resulting in a faster reaction rate. After 5 h at 120 °C, the hydrolyzed membrane is still flexible and strong. As shown in Table 2, the mechanical properties of carboxylated PIMs are only slightly lower than those of PIM-1.

Thermal analyses of carboxylated PIMs and PIM-1 are summarized in Table 2. None of the polymers have a discernible T_g in the measured range of 50 to 350 °C. TGA experiments showed that all carboxylated PIMs have good thermal stabilities and the actual onset temperature of decomposition in nitrogen is above 250 °C. There is also a trend between T_d and the degree of hydrolysis. In general, nitrile-containing polymers have high thermal stability, likely due to strong dipolar interactions. Table 2 shows that with increasing degree of hydrolysis, the T_d onset decreased. However, all carboxylated PIMs still show very good thermal stability, even after complete hydrolysis of nitrile to carboxylic acid groups.

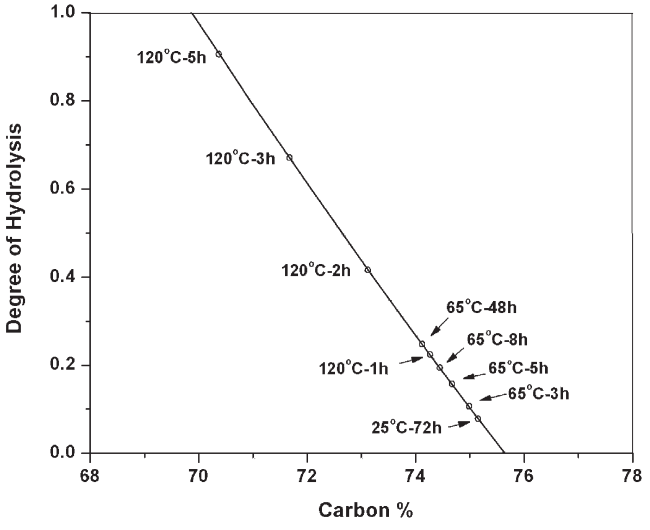

Figure 3. Relationship between the degree of hydrolysis and the carbon content for carboxylated PIMs.

PIM-1 is readily soluble in tetrahydrofuran (THF), dichloromethane (CH_2Cl_2), and chloroform ($CHCl_3$), but insoluble in polar aprotic solvents such as dimethylformamide (DMF), dimethylacetamide (DMAc), and *N*-methylpyrrolidone (NMP). After partial hydrolysis at 120 °C, the hydrolyzed PIM-1 membrane was no longer soluble in CH_2Cl_2 and $CHCl_3$, but it was still partially soluble in THF. With further hydrolysis, THF was a nonsolvent and DMF, DMAc, and NMP were good solvents for the hydrolyzed PIM-1 membrane, indicating that the carboxylated PIMs still have good processability.

Gas permeabilities and selectivities of carboxylated PIMs having different degrees of hydrolysis follow a trade-off relationship similar to that observed for many glassy or rubbery polymers. In general, higher permeability is gained at the cost of lower selectivity and vice versa. Pure-gas permeability coefficients (P) were measured on polymer dense films of PIM-1 and carboxylated PIMs for O_2, N_2, H_2, He, and CO_2. A summary of these P values and ideal selectivities for various gas pairs are shown in Table 1. Gas permeability and selectivity of PIM-1 are known to be very sensitive to film preparation conditions and pretreatment.[24] There is variation between the previously reported permeability data and the present data for PIM-1, as shown in Figure 5.

It is likely that this difference arises from the post-treatment protocol for the membranes. Different from previous work, the hydrolyzed PIM membranes were treated by first boiling in water

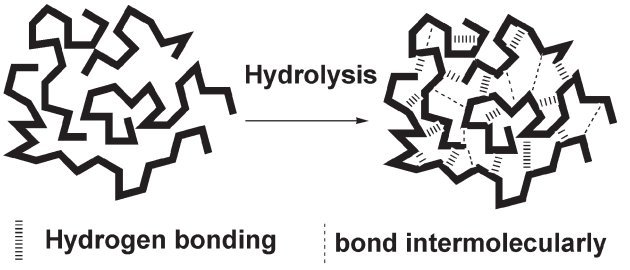

Figure 4. Representation of hydrogen or intermolecular bonding in carboxylated PIMs.

Table 1. Gas Permeabilities and Ideal Selectivities of Carboxylated PIMs and PIM-1

polymers	carbon elemental analyses	P (Barrer)[a]					α[b]			
		O_2	N_2	He	H_2	CO_2	O_2/N_2	CO_2/N_2	He/N_2	H_2/N_2
PIM-1		1790	727	1368	3580	8310	2.5	11	1.9	4.9
25 °C, 0.5 h		1555	615	1284	3143	6715	2.5	11	2.0	5.1
25 °C, 5 h		1384	523	1204	2885	6294	2.7	12	2.3	5.5
25 °C, 24 h		1107	385	1022	2510	5133	2.9	13	2.7	6.5
25 °C, 48 h		990	338	990	2265	4775	2.9	14	2.9	6.7
25 °C, 72 h	75.13	784	282	837	1902	3924	2.8	14	3.0	6.8
65 °C, 1 h		1053	369	980	2370	4586	2.9	12	2.6	6.4
65 °C, 3 h	74.97	842	284	870	2247	3965	3.0	14	3.1	7.9
65 °C, 5 h	74.65	600	187	627	1720	2990	3.2	16	4.2	9.3
65 °C, 8 h	74.44	540	164	680	1521	2656	3.3	16	4.2	9.3
65 °C, 16 h		470	138	607	1407	2305	3.4	17	4.4	10
65 °C, 24 h		400	110	523	1256	1962	3.6	18	4.8	11
65 °C, 48 h	74.12	281	70	391	917	1521	4.0	22	5.6	13
120 °C, 1 h	74.29	534	162	616	1540	2543	3.3	16	3.8	9.5
120 °C, 2 h	73.10	351	100	484	1152	2060	3.5	21	4.9	12
120 °C, 3 h	71.67	201	48	260	630	1056	4.2	22	5.4	13
120 °C, 5 h	70.30	110	24	153	408	620	4.6	26	6.3	17

[a] Permeability coefficients measured at 25 °C and 50 psig feed pressure. One Barrer = 10^{-10} [cm^3(STP)·cm]/(cm^2·s·cmHg). [b] Ideal selectivity $\alpha = (P_a)/(P_b)$.

Table 2. Mechanical and Thermal Properties of Carboxylated PIMs

polymers	T_d (°C)[a]	T_d (°C)[b]	T_{d5} (°C)[c]	RW (%)[d]	tensile stress at break (MPa)	tensile strain at break (%)
PIM-1	384	505	495	77	45.1	7.2
120 °C, 1 h	309	485	472	70	45.2	7.0
120 °C, 2 h	291	485	460	69	47.2	6.7
120 °C, 3 h	282	475	448	68	58.7	6.5
120 °C, 5 h	258	390	406	63	39.6	3.7

[a] Actual onset temperature of decomposition. [b] Extrapolated onset temperature of decomposition measured by TGA. [c] 5% weight loss temperature measured by TGA. [d] Residue weight at 600 °C under N_2.

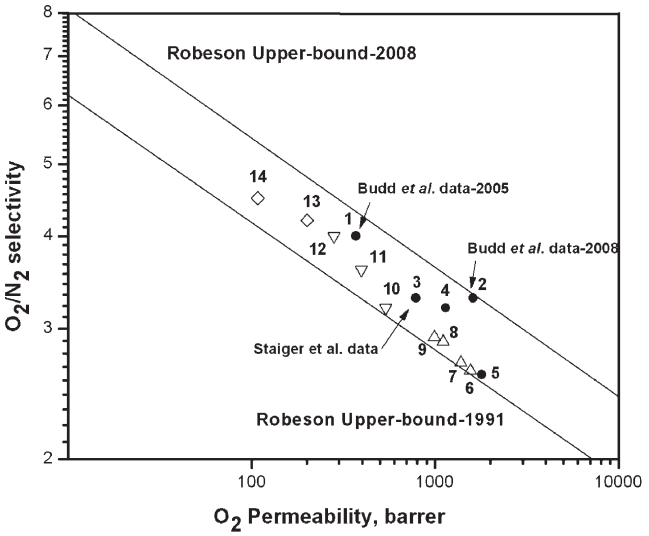

Figure 5. Relationship between O_2 permeability and O_2/N_2 selectivity for carboxylated PIMs and PIM-1. PIM-1 (●): 1, reported by Budd et al. (2005) at 200 mbar (2.90 psia) feed pressure at 30 °C;[16] 2, reported by Budd et al. (2008) at 1 atm (14.7 psig) feed pressure at 23 °C;[24] 3, reported by Staiger et al. at 4 atm (58.8 psia) feed pressure 35 °C;[25] 4, reported by Du et al. at 4.4 atm (50 psig) feed pressure 25 °C;[20] 5, the membrane was prepared using an identical acid post-treatment procedure to those used for preparing the carboxylated PIMs and tested at 4.4 atm (50 psig) feed pressure at 25 °C. Carboxylated PIMs at 4.4 atm (50 psig) feed pressure at 25 °C (△) [6, 25 °C, 0.5 h; 7, 25 °C, 5 h; 8, 25 °C, 24 h; 9, 25 °C, 48 h]. (▽) [10, 65 °C, 8 h; 11, 65 °C, 24 h; 12, 65 °C, 48 h]. (◇) [13, 120 °C, 3 h; 14, 120 °C, 5 h].

(with HCl, pH 4 to 5) to remove sodium hydroxide and salts. After several washes in water, they were soaked in methanol and then allowed to dry naturally. Finally, the membranes were dried in a vacuum oven for 24 h by gradually increasing the temperature from ambient to 100 °C. For comparison, a PIM-1 membrane of the present study was treated identically. The permeabilities of the water-treated PIM-1 membrane for all gases are higher than those of previous reports, whereas selectivities are lower, illustrating the strong effect of processing history on performance.[16,20,24,25] The O_2/N_2 selectivities for PIM-1 are above the Robeson upper bound (1991), with expected "trade-off" behavior between permeability and selectivity, as shown in Figure 5.[26,27] All carboxylated PIMs exhibited higher O_2/N_2 selectivity compared with PIM-1 (no. 5 is PIM-1, which was fabricated and tested under the same conditions) coupled to reductions in gas permeabilities. From the viewpoint of molecular modeling analyses by using HyperChem 7.0 software, the interchain distance of the polymer is not extensively changed by the introduction of carboxylic acid groups into the PIM. Nitrile and carboxylic acid groups are similarly sized small side groups, which do not have a large effect on interchain space filling. However, strong interchain hydrogen bonds may somewhat rearrange the chains, build up a network structure and enhance the rigidity of polymer chains, which would lead to lower permeability and higher selectivity. This hypothesis is in good agreement with the FTIR spectral analysis. The intrinsic intermolecular force of these carboxylated PIMs is expected to be independent of processing. The number of hydrogen bonding network structures can be controlled by temperature and reaction time. Therefore, postmodification of PIM-1 by various hydrolysis conditions is a simple method to adjust or tune the gas permeability and selectivity.

Conclusions

Carboxylated PIMs were prepared by simple hydrolysis of PIM-1 films using sodium hydroxide solution. The degree of hydrolysis and structures were characterized by FTIR, ^{1}H NMR, and carbon elemental analysis. The fully hydrolyzed PIM-1 film, dicarboxylated-PIM, maintained good processability since it could be dissolved in polar aprotic solvents such as DMF, DMAc, and NMP. All carboxylated-PIM membranes derived from different degrees of hydrolysis had good mechanical properties and thermal stabilities while showing evident decreases in O_2, N_2, He, H_2, and CO_2 permeabilities and significant increases in pure-gas selectivities against N_2. Therefore, the postmodification nitrile hydrolysis of the PIM-1 approach expands the spectrum of PIM materials and provides a means to tune selectivity and permeability by varying hydrolysis reaction conditions, which can be feasibly applied to industrial application.

Acknowledgment. This work was supported primarily by the Climate Change Technology and Innovation Initiative, Greenhouse Gas project (CCTII, GHG), Natural Resources Canada (NRCan). Partial support was also provided by the U.S. Department of Energy (SBIR contract number DE-FG02-05ER84243). We are grateful to Mr. Floyd N. Toll of the National Research Council for the mechanical properties and elemental analysis testing.

References and Notes

(1) Davankov, V. A.; Tsyurupa, M. P. *React. Polym.* **1990**, *13*, 27–42.
(2) Tsyurupa, M. P.; Davankov, V. A. *React. Funct. Polym.* **2002**, *53*, 193–203.
(3) Webster, O. W.; Gentry, F. P.; Farlee, R. D.; Smart, B. E. *Makromol.Chem., Macromol. Symp.* **1992**, *54*, 477–482.
(4) Urban, C.; McCord, E. F.; Webster, O. W.; Abrams, L.; Long, H. W.; Gaede, H.; Tang, P.; Pines, A. *Chem. Mater.* **1995**, *7*, 1325–1332.
(5) Wood, C. D.; Tan, B.; Trewin, A.; Niu, H. J.; Bradshaw, D.; Rosseinsky, M. J.; Khimyak, Y. Z.; Campbell, N. L.; Kirk, R.; Stockel, E.; Cooper, A. I. *Chem. Mater.* **2007**, *19*, 2034–2048.
(6) Masuda, T.; Isobe, E.; Higashimura, T.; Takada, K. *J. Am. Chem. Soc.* **1983**, *105*, 7473–7474.
(7) Nagai, K.; Masuda, T.; Nakagawa, T.; Freeman, B. D.; Pinnau, I. *Prog. Polym. Sci.* **2001**, *26*, 721–798.
(8) Tanaka, K.; Okano, M.; Toshino, H.; Kita, H.; Okamoto, K. I. *J. Polym.Sci., Polym. Phys.* **1992**, *30*, 907–914.
(9) Weber, J.; Su, Q.; Antonietti, M.; Thomas, A. *Macromol. Rapid Commun.* **2007**, *28*, 1871–1876.
(10) Yu, A.; Shantarovich, V.; Merkel, T. C.; Bondar, V. I.; Freeman, B. D.; Yampolskii, Y. *Macromolecules* **2002**, *35*, 9513–9522.
(11) Pinnau, I.; Toy, L. G. *J. Membr. Sci.* **1996**, *116*, 199–209.
(12) Dai, Y.; Guiver, M. D.; Robertson, G. P.; Kang, Y. S.; Lee, K. J.; Jho, J. Y. *Macromolecules* **2004**, *37*, 1403–1410.
(13) Budd, P. M.; Ghanem, B. S.; Makhseed, S.; McKeown, N. B.; Msayib, K. J.; Tattershall, C. E. *Chem. Commun.* **2004**, 230–231.
(14) Budd, P. M.; Elabas, E. S.; Ghanem, B. S.; Makhseed, S.; McKeown, N. B.; Msayib, K. J.; Tattershall, C. E.; Wong, D. *Adv. Mater.* **2004**, *16*, 456–459.
(15) McKeown, N. B.; Budd, P. M.; Msayib, K.; Ghanem, B. S. Microporous Polymer Material. WO Patent 012397 A2, **2005**.
(16) Budd, P. M.; Msayib, K. J.; Tattershall, C. E.; Reynolds, K. J.; McKeown, N. B.; Fritsch, D. *J. Membr. Sci.* **2005**, *251*, 263–269.
(17) McKeown, N. B.; Budd, P. M.; Msayib, K. J.; Ghanem, B. S.; Kingston, H. J.; Tattershall, C. E.; Makhseed, S.; Reynolds, K. J.; Fritsch, D. *Chem.—Eur. J.* **2005**, *11*, 2610–2620.

(18) Ghanem, B. S.; McKeown, N. B; Budd, P. M.; Fritsch, D. *Macromolecules* **2008**, *41*, 1640–1646.
(19) Carta, M.; Msayib, K. J.; Budd, P. M.; McKeown, N. B. *Org. Lett.* **2008**, *10*, 2641–2643.
(20) Du, N.; Robertson, G. P.; Song, J.; Pinnau, I.; Thomas, S.; Guiver, M. D. *Macromolecules* **2008**, *41*, 9656–9662.
(21) Du, N.; Robertson, G. P.; Pinnau, I.; Thomas, S.; Guiver, M. D. *Macromol. Rapid Commun.* **2009**, *30*, 584–588.
(22) Silverstein, R. M.; Webster, F. X. *Spectrometric Identification of Organic Compounds*, 6th ed.; John Wiley & Sons: Hoboken, NJ; (a) pp 163−166, (b) 95.
(23) Clerc, P.; Simon, S. *Table of Spectral Data for Structure Determination of Organic Compounds*; Springer Verlag: Berlin, 1983; pp I165, I45.
(24) Budd, P. M.; McKeown, N. B.; Ghanem, B. S.; Msayib, K. J.; Fritsch, D.; Starannikova, L.; Belov, N.; Sanfirova, O.; Yampolskii, Y.; Shantarovich, V. J. *Membr. Sci.* **2008**, *325*, 851–860.
(25) Staiger, C. L.; Pas, S. J.; Hill, A. J.; Cornelius, C. J. *Chem. Mater.* **2008**, *20*, 2606–2008.
(26) Robeson, L. M. *J. Membr. Sci.* **1991**, *62*, 165–185.
(27) Robeson, L. M. *J. Membr. Sci.* **2008**, *320*, 390–400.